EUROPEAN ORGANIZATION FOR NUCLEAR RESEARCH

CERN-PPE/97-024
24 February 1997

Measurement of the Branching Fraction for $D^0 \to K^-\pi^+$

The ALEPH Collaboration*

Abstract

The branching fraction for $D^0 \to K^-\pi^+$ is measured with the statistics collected by ALEPH from 1991 to 1994. The method is based on the comparison between the rate for the reconstructed $D^{*+} \to D^0\pi^+$, $D^0 \to K^-\pi^+$ decay chain and the rate for inclusive soft pion production at low transverse momentum with respect to the nearest jet. The result is $B(D^0 \to K^-\pi^+) = (3.90 \pm 0.09 \pm 0.12)\%$

(To be submitted to Phys. Lett. B)

*See the following pages for the list of authors.

The ALEPH Collaboration

R. Barate, D. Buskulic, D. Decamp, P. Ghez, C. Goy, J.-P. Lees, A. Lucotte, M.-N. Minard, J.-Y. Nief, B. Pietrzyk

Laboratoire de Physique des Particules (LAPP), IN^{2}P^3-CNRS, 74019 Annecy-le-Vieux Cedex, France

M.P. Casado, M. Chmeissani, P. Comas, J.M. Crespo, M. Delfino, E. Fernandez, M. Fernandez-Bosman, Ll. Garrido,[15] A. Juste, M. Martinez, R. Miquel, Ll.M. Mir, S. Orteu, C. Padilla, I.C. Park, A. Pascual, J.A. Perlas, I. Riu, F. Sanchez, F. Teubert

Institut de Fisica d'Altes Energies, Universitat Autonoma de Barcelona, 08193 Bellaterra (Barcelona), Spain[7]

A. Colaleo, D. Creanza, M. de Palma, G. Gelao, G. Iaselli, G. Maggi, M. Maggi, N. Marinelli, S. Nuzzo, A. Ranieri, G. Raso, F. Ruggieri, G. Selvaggi, L. Silvestris, P. Tempesta, A. Tricomi,[3] G. Zito

Dipartimento di Fisica, INFN Sezione di Bari, 70126 Bari, Italy

X. Huang, J. Lin, Q. Ouyang, T. Wang, Y. Xie, R. Xu, S. Xue, J. Zhang, L. Zhang, W. Zhao

Institute of High-Energy Physics, Academia Sinica, Beijing, The People's Republic of China[8]

D. Abbaneo, R. Alemany, U. Becker, A.O. Bazarko,[20] P. Bright-Thomas, M. Cattaneo, F. Cerutti, H. Drevermann, R.W. Forty, M. Frank, R. Hagelberg, J. Harvey, P. Janot, B. Jost, E. Kneringer, J. Knobloch, I. Lehraus, G. Lutters, P. Mato, A. Minten, L. Moneta, A. Pacheco, J.-F. Pusztaszeri, F. Ranjard, P. Rensing,[12] G. Rizzo, L. Rolandi, D. Schlatter, M. Schmitt, O. Schneider, W. Tejessy, I.R. Tomalin, H. Wachsmuth, A. Wagner

European Laboratory for Particle Physics (CERN), 1211 Geneva 23, Switzerland

Z. Ajaltouni, A. Barrès, C. Boyer, A. Falvard, C. Ferdi, P. Gay, C . Guicheney, P. Henrard, J. Jousset, B. Michel, S. Monteil, J-C. Montret, D. Pallin, P. Perret, F. Podlyski, J. Proriol, P. Rosnet, J.-M. Rossignol

Laboratoire de Physique Corpusculaire, Université Blaise Pascal, IN^{2}P^3-CNRS, Clermont-Ferrand, 63177 Aubière, France

T. Fearnley, J.B. Hansen, J.D. Hansen, J.R. Hansen, P.H. Hansen, B.S. Nilsson, B. Rensch, A. Wäänänen

Niels Bohr Institute, 2100 Copenhagen, Denmark[9]

G. Daskalakis, A. Kyriakis, C. Markou, E. Simopoulou, I. Siotis, A. Vayaki

Nuclear Research Center Demokritos (NRCD), Athens, Greece

A. Blondel, G. Bonneaud, J.C. Brient, P. Bourdon, A. Rougé, M. Rumpf, A. Valassi,[6] M. Verderi, H. Videau

Laboratoire de Physique Nucléaire et des Hautes Energies, Ecole Polytechnique, IN^{2}P^3-CNRS, 91128 Palaiseau Cedex, France

D.J. Candlin, M.I. Parsons

Department of Physics, University of Edinburgh, Edinburgh EH9 3JZ, United Kingdom[10]

E. Focardi, G. Parrini, K. Zachariadou

Dipartimento di Fisica, Università di Firenze, INFN Sezione di Firenze, 50125 Firenze, Italy

M. Corden, C. Georgiopoulos, D.E. Jaffe

Supercomputer Computations Research Institute, Florida State University, Tallahassee, FL 32306-4052, USA [13,14]

A. Antonelli, G. Bencivenni, G. Bologna,[4] F. Bossi, P. Campana, G. Capon, D. Casper, V. Chiarella, G. Felici, P. Laurelli, G. Mannocchi,[5] F. Murtas, G.P. Murtas, L. Passalacqua, M. Pepe-Altarelli

Laboratori Nazionali dell'INFN (LNF-INFN), 00044 Frascati, Italy

L. Curtis, S.J. Dorris, A.W. Halley, I.G. Knowles, J.G. Lynch, V. O'Shea, C. Raine, J.M. Scarr, K. Smith, P. Teixeira-Dias, A.S. Thompson, E. Thomson, F. Thomson, R.M. Turnbull

Department of Physics and Astronomy, University of Glasgow, Glasgow G12 8QQ,United Kingdom[10]

C. Geweniger, G. Graefe, P. Hanke, G. Hansper, V. Hepp, E.E. Kluge, A. Putzer, M. Schmidt, J. Sommer, K. Tittel, S. Werner, M. Wunsch

Institut für Hochenergiephysik, Universität Heidelberg, 69120 Heidelberg, Fed. Rep. of Germany[16]

R. Beuselinck, D.M. Binnie, W. Cameron, P.J. Dornan, M. Girone, S. Goodsir, E.B. Martin, A. Moutoussi, J. Nash, J.K. Sedgbeer, A.M. Stacey, M.D. Williams

Department of Physics, Imperial College, London SW7 2BZ, United Kingdom[10]

G. Dissertori, P. Girtler, D. Kuhn, G. Rudolph

Institut für Experimentalphysik, Universität Innsbruck, 6020 Innsbruck, Austria[18]

A.P. Betteridge, C.K. Bowdery, P. Colrain, G. Crawford, A.J. Finch, F. Foster, G. Hughes, T. Sloan, M.I. Williams

Department of Physics, University of Lancaster, Lancaster LA1 4YB, United Kingdom[10]

A. Galla, I. Giehl, A.M. Greene, C. Hoffmann, K. Jakobs, K. Kleinknecht, G. Quast, B. Renk, E. Rohne, H.-G. Sander, P. van Gemmeren, C. Zeitnitz

Institut für Physik, Universität Mainz, 55099 Mainz, Fed. Rep. of Germany[16]

J.J. Aubert, C. Benchouk, A. Bonissent, G. Bujosa, D. Calvet, J. Carr, P. Coyle, C. Diaconu, F. Etienne, N. Konstantinidis, O. Leroy, F. Motsch, P. Payre, D. Rousseau, M. Talby, A. Sadouki, M. Thulasidas, K. Trabelsi

Centre de Physique des Particules, Faculté des Sciences de Luminy, IN^{2}P^3-CNRS, 13288 Marseille, France

M. Aleppo, F. Ragusa[2]

Dipartimento di Fisica, Università di Milano e INFN Sezione di Milano, 20133 Milano, Italy

R. Berlich, W. Blum, V. Büscher, H. Dietl, F. Dydak,[2] G. Ganis, C. Gotzhein, H. Kroha, G. Lütjens, G. Lutz, W. Männer, H.-G. Moser, R. Richter, A. Rosado-Schlosser, S. Schael, R. Settles, H. Seywerd, R. St. Denis, H. Stenzel, W. Wiedenmann, G. Wolf

Max-Planck-Institut für Physik, Werner-Heisenberg-Institut, 80805 München, Fed. Rep. of Germany[16]

J. Boucrot, O. Callot,[2] S. Chen, Y. Choi,[21] A. Cordier, M. Davier, L. Duflot, J.-F. Grivaz, Ph. Heusse, A. Höcker, A. Jacholkowska, M. Jacquet, D.W. Kim,[24] F. Le Diberder, J. Lefrançois, A.-M. Lutz, I. Nikolic, M.-H. Schune, S. Simion, E. Tournefier, J.-J. Veillet, I. Videau, D. Zerwas

Laboratoire de l'Accélérateur Linéaire, Université de Paris-Sud, IN^{2}P^3-CNRS, 91405 Orsay Cedex, France

P. Azzurri, G. Bagliesi, G. Batignani, S. Bettarini, C. Bozzi, G. Calderini, M. Carpinelli, M.A. Ciocci, V. Ciulli, R. Dell'Orso, R. Fantechi, I. Ferrante, L. Foà,[1] F. Forti, A. Giassi, M.A. Giorgi, A. Gregorio, F. Ligabue, A. Lusiani, P.S. Marrocchesi, A. Messineo, F. Palla, G. Sanguinetti, A. Sciabà, P. Spagnolo, J. Steinberger, R. Tenchini, G. Tonelli,[19] C. Vannini, A. Venturi, P.G. Verdini

Dipartimento di Fisica dell'Università, INFN Sezione di Pisa, e Scuola Normale Superiore, 56010 Pisa, Italy

G.A. Blair, L.M. Bryant, J.T. Chambers, Y. Gao, M.G. Green, T. Medcalf, P. Perrodo, J.A. Strong, J.H. von Wimmersperg-Toeller

Department of Physics, Royal Holloway & Bedford New College, University of London, Surrey TW20 OEX, United Kingdom[10]

D.R. Botterill, R.W. Clifft, T.R. Edgecock, S. Haywood, P. Maley, P.R. Norton, J.C. Thompson, A.E. Wright

Particle Physics Dept., Rutherford Appleton Laboratory, Chilton, Didcot, Oxon OX11 OQX, United Kingdom[10]

B. Bloch-Devaux, P. Colas, S. Emery, W. Kozanecki, E. Lançon, M.C. Lemaire, E. Locci, P. Perez, J. Rander, J.-F. Renardy, A. Roussarie, J.-P. Schuller, J. Schwindling, A. Trabelsi, B. Vallage

CEA, DAPNIA/Service de Physique des Particules, CE-Saclay, 91191 Gif-sur-Yvette Cedex, France[17]

S.N. Black, J.H. Dann, R.P. Johnson, H.Y. Kim, A.M. Litke, M.A. McNeil, G. Taylor

Institute for Particle Physics, University of California at Santa Cruz, Santa Cruz, CA 95064, USA[22]

C.N. Booth, R. Boswell, C.A.J. Brew, S. Cartwright, F. Combley, M.S. Kelly, M. Lehto, W.M. Newton, J. Reeve, L.F. Thompson

Department of Physics, University of Sheffield, Sheffield S3 7RH, United Kingdom[10]

A. Böhrer, S. Brandt, G. Cowan, C. Grupen, P. Saraiva, L. Smolik, F. Stephan

Fachbereich Physik, Universität Siegen, 57068 Siegen, Fed. Rep. of Germany[16]

M. Apollonio, L. Bosisio, R. Della Marina, G. Giannini, B. Gobbo, G. Musolino

Dipartimento di Fisica, Università di Trieste e INFN Sezione di Trieste, 34127 Trieste, Italy

J. Rothberg, S. Wasserbaech

Experimental Elementary Particle Physics, University of Washington, WA 98195 Seattle, U.S.A.

S.R. Armstrong, E. Charles, P. Elmer, D.P.S. Ferguson, Y.S. Gao,[23] S. González, T.C. Greening, O.J. Hayes, H. Hu, S. Jin, P.A. McNamara III, J.M. Nachtman, J. Nielsen, W. Orejudos, Y.B. Pan, Y. Saadi, I.J. Scott, J. Walsh, Sau Lan Wu, X. Wu, J.M. Yamartino, G. Zobernig

Department of Physics, University of Wisconsin, Madison, WI 53706, USA[11]

---

[1]Now at CERN, 1211 Geneva 23, Switzerland.
[2]Also at CERN, 1211 Geneva 23, Switzerland.
[3]Also at Dipartimento di Fisica, INFN, Sezione di Catania, Catania, Italy.
[4]Also Istituto di Fisica Generale, Università di Torino, Torino, Italy.
[5]Also Istituto di Cosmo-Geofisica del C.N.R., Torino, Italy.
[6]Supported by the Commission of the European Communities, contract ERBCHBICT941234.
[7]Supported by CICYT, Spain.
[8]Supported by the National Science Foundation of China.
[9]Supported by the Danish Natural Science Research Council.
[10]Supported by the UK Particle Physics and Astronomy Research Council.
[11]Supported by the US Department of Energy, grant DE-FG0295-ER40896.
[12]Now at Dragon Systems, Newton, MA 02160, U.S.A.
[13]Supported by the US Department of Energy, contract DE-FG05-92ER40742.
[14]Supported by the US Department of Energy, contract DE-FC05-85ER250000.
[15]Permanent address: Universitat de Barcelona, 08208 Barcelona, Spain.
[16]Supported by the Bundesministerium für Bildung, Wissenschaft, Forschung und Technologie, Fed. Rep. of Germany.
[17]Supported by the Direction des Sciences de la Matière, C.E.A.
[18]Supported by Fonds zur Förderung der wissenschaftlichen Forschung, Austria.
[19]Also at Istituto di Matematica e Fisica, Università di Sassari, Sassari, Italy.
[20]Now at Princeton University, Princeton, NJ 08544, U.S.A.
[21]Permanent address: Sung Kyun Kwan University, Suwon, Korea.
[22]Supported by the US Department of Energy, grant DE-FG03-92ER40689.
[23]Now at Harvard University, Cambridge, MA 02138, U.S.A.
[24]Permanent address: Kangnung National University, Kangnung, Korea.

1 Introduction

The decay mode $D^0 \to K^-\pi^+$ plays an important role in heavy flavour physics[1]. It is often used to normalize the other decay modes of the D^0 meson. Furthermore the precision of such a measurement is particularly important since it is a limiting factor in measurements concerning B meson decays.

The method used here to extract the branching fraction is the one pioneered by the HRS experiment [1]. It makes use of the very small Q value ($\approx$ 6 MeV/c^2) of the $D^{*+} \to D^0\pi^+$ decay or, equivalently, of the low momentum of the pion in the D^{*+} rest frame, $p^* \sim 40$ MeV/c. The π^+ has its transverse momentum relative to D^{*+} line of flight bounded by this value and it takes a small fraction [$\mathcal{O}\,(m_\pi/m_{D^*} = 0.07)$] of the longitudinal momentum. For this reason throughout this paper it will be called a soft pion and referred to as π_s.

The rate of $D^{*+} \to D^0\pi^+$ decays is obtained by approximating the D^{*+} direction with the direction of the jet containing the π_s, and measuring the excess of pions at low transverse momentum with respect to the jet axis. The rate of $D^{*+} \to D^0\pi^+$, $D^0 \to K^-\pi^+$ decays is then measured by fully reconstructing the decay chain with high efficiency. The branching fraction is derived from the two rates. The first measurement is referred to as 'inclusive' and the second as 'exclusive' in the following.

2 ALEPH Detector and Data Selection

This study uses data recorded from 1991 to 1994 with the ALEPH detector at the LEP e^+e^- storage ring. A detailed description of the detector can be found in Ref. [2, 3]. In this section only the features relevant to this study are given. The tracking uses a set of three concentric detectors: a large time projection chamber (TPC) surrounding a drift chamber, called the inner tracking chamber (ITC), and, closest to the interaction region, a silicon vertex detector (VDET). This whole tracking system is immersed in a 1.5 T magnetic field produced by a superconducting solenoid. A global fit to the TPC, ITC and VDET coordinates allows track momenta to be measured with an accuracy of $\delta p_T/p_T = 6 \times 10^{-4} p_T$ (GeV/c)$^{-1} \oplus 5 \times 10^{-3}$ [3].

The data sample consists of about three million hadronic Z decays selected as described in Ref. [4]. It is required that they contain at least five charged tracks of momentum above 0.2 GeV/c and polar angle θ, with respect to the beam axis, satisfying $|\cos\theta| < 0.95$. Their distance of closest approach to the interaction point must be less than 10 cm along the beam axis and less than 2 cm in the transverse plane. The sum of the momenta of all tracks meeting these conditions must be greater than 10% of the centre-of-mass energy.

3 Inclusive Analysis of the Decay $D^{*+} \to D^0\pi_s^+$

In this analysis, as in Ref. [1, 5, 6, 7, 8], no attempt is made to reconstruct the D^0 decay. The signal relies only on the observed transverse momentum distribution of charged tracks

[1] charge-conjugate modes are implied throughout this paper

within a momentum range kinematically accessible for the soft pion from a D^{*+} decay, that is, between 1 and 4 GeV/c.

In order to estimate the D^{*+} direction, even if the D^0 is not reconstructed, the axis of the nearest jet to the π_s is used. Jets are reconstructed from charged tracks and neutral energy in the calorimeters [3], according to the scaled-invariant-mass algorithm [9]. The jet resolution parameter $Y_{\rm cut}$ is fixed to 0.0024, corresponding to a jet mass of about 4 GeV/c^2; this value minimizes the uncertainty on the direction of the D^{*+} and so increases the separation power for the signal from the background. The polar angle of the jet, $\theta_{\rm jet}$, must satisfy $|\cos\theta_{\rm jet}| < 0.85$ in order to select jets with well measured axis. The jet containing the soft pion must have at least two additional charged tracks.

Figure 1a) shows the $p_{\rm T}^2$ distributions of the selected tracks in six momentum bins of width 0.5 GeV/c. A clear excess of events can be seen at low $p_{\rm T}^2$. Two main sources contribute to the signal at the LEP energies: the decay $Z \to c\bar{c}$, where a c quark hadronizes, and the decay $Z \to b\bar{b}$, where a b hadron subsequently decays into charm. The gluon splitting $g \to c\bar{c}$ and $g \to b\bar{b}$ events give a small contribution and are taken into account.

The overall $p_{\rm T}^2$ distribution of the signal depends on the relative amount of the three contributions:

$$F_{\rm sig}(p_{\rm T}^2) = f_{\rm c}\mathcal{P}_{\rm c}(p_{\rm T}^2) + f_{\rm b}\mathcal{P}_{\rm b}(p_{\rm T}^2) + f_{\rm g}\mathcal{P}_{\rm g}(p_{\rm T}^2) \ .$$

The fractions of D^{*+} events produced from c quarks, $f_{\rm c}$, from b quarks, $f_{\rm b}$, and from gluon splitting, $f_{\rm g}$, are estimated for each momentum bin. The estimate of the relative contributions of c and b events uses the ALEPH measured values [10] of the ratio of the probabilities for a $b\bar{b}$ or a $c\bar{c}$ events to give a $D^{*\pm}$, $P(b \to D^{*+})/P(c \to D^{*+}) = 0.87^{+0.15}_{-0.13}$, with $R_{\rm b} = \Gamma_{Z\to b\bar{b}}/\Gamma_{Z\to {\rm had}}$ and $R_{\rm c} = \Gamma_{Z\to c\bar{c}}/\Gamma_{Z\to {\rm had}}$ fixed to the Standard Model values. The ratio of the numbers of $D^{*\pm}$ from $g \to c\bar{c}$ and from primary charm quarks is $\bar{n}_{g\to c\bar{c}}/R_{\rm c} = (13.3 \pm 3.3)\%$, where $\bar{n}_{g\to c\bar{c}}$ is taken from Ref. [11]. It is assumed that the probability to hadronize into a D^{*+} is the same for gluon splitting and direct charm production. The ratio between gluon splitting into $b\bar{b}$ and $c\bar{c}$ is estimated to be $\bar{n}_{g\to b\bar{b}}/(\bar{n}_{g\to c\bar{c}} + \bar{n}_{g\to b\bar{b}}) = 0.132 \pm 0.047$ according to different Monte Carlo models [12]. This translates into an additional $(1.8 \pm 0.8)\%$ fraction of D^{*+}'s from gluon splitting with respect to primary charm. The dependence on momentum for all processes is predicted from the Monte Carlo using the fragmentation functions parameterized by the Peterson function [13] with the ALEPH measured values of the fragmentation parameters $\varepsilon_c = (52^{+13}_{-11}) \times 10^{-3}$ [10] and $\varepsilon_b = (3.2 \pm 1.7) \times 10^{-3}$ [14]. The typical contribution of the gluon splitting process to the selected D^{*+} sample is about 1%.

The shapes of the $p_{\rm T}^2$ distributions, $\mathcal{P}_{\rm c}(p_{\rm T}^2)$, $\mathcal{P}_{\rm b}(p_{\rm T}^2)$ and $\mathcal{P}_{\rm g}(p_{\rm T}^2)$ are taken from Monte Carlo after detector simulation and the same event reconstruction as used for the real data. The $p_{\rm T}^2$ distributions depend on the π_s decay angle with respect to the D^{*+} line of flight in the D^{*+} rest frame, θ_π^*, and on the angle $\theta_{\rm D^{*+},jet}$ between the D^{*+} and the jet. These two quantities are measured from data by using the fully reconstructed decay chains $D^{*+} \to D^0\pi^+$, $D^0 \to K^-\pi^+$. The θ_π^* distribution depends on the spin alignment of the D^{*+}. In $c\bar{c}$ events the decay angle distribution follows a $(1 + \alpha\cos^2\theta_\pi^*)$ probability function, where the parameter α is linked to the alignment. In this sample the measured value of the parameter is $\alpha = 0.25 \pm 0.15$, where the uncertainty includes the statistical error and systematic error due to background subtraction and efficiency computation.

Since in the Monte Carlo the alignment is set to zero, the resulting small correction factors are applied to the expected fraction of charm events in each momentum bin and to the expected $p_{\rm T}^2$ shapes $\mathcal{P}_{\rm c}(p_{\rm T}^2)$. In $\rm b\bar{b}$ events the $\cos\theta_\pi^*$ distribution is expected to be flat since the helicity axis is the direction of the $\rm D^{*+}$ in the b hadron rest frame. Figure 2 shows the measured $\theta_{\rm D^{*+},jet}$ distribution together with the Monte Carlo prediction with the flavour composition as expected from the measurement described in the previous paragraph. Correction factors are applied to all the $\mathcal{P}(p_{\rm T}^2)$ shapes to account for the observed differences between data and Monte Carlo.

To extract the number of observed $\rm D^{*+} \to D^0\pi^+$ decays per momentum bin, $N_{\rm D^{*+}\to D^0\pi^+}$, a fit is performed to each $p_{\rm T}^2$ distribution with the function

$$\frac{dN}{dp_{\rm T}^2} = N_{\rm D^{*+}\to D^0\pi^+} F_{\rm sig}(p_{\rm T}^2) + F_{\rm bg}(p_{\rm T}^2) \ .$$

The background shape is parameterized as follows:

$$F_{\rm bg}(p_{\rm T}^2) = \frac{a}{1 + bp_{\rm T}^2 + c(p_{\rm T}^2)^2 + d(p_{\rm T}^2)^3} \ ,$$

where the parameters a, b, c and d depend on the momentum bin. This function is tested on a Monte Carlo sample from which the π_s tracks are removed, for different values of $Y_{\rm cut}$ and for all momentum bins. In this test $N_{\rm D^{*+}\to D^0\pi^+}$ represents the number of π_s's found and should be zero for the sample used. The deviation from zero, normalized to the fitted number of background tracks, is taken as an additional background component to be subtracted from the results of the fits on the data sample. The uncertainty from this source is taken to be 100%. This effect is due to the slight inadequacy of the simple parameterization used to describe the background shapes. In fact the $p_{\rm T}^2$ distributions of tracks coming from two-body decays are in general peaked at a value that depends on the Q value of the decay. For example, tracks coming directly from L = 1 meson states produce a Jacobian peak at $p_{\rm T}^2 \approx 0.12$ $(\rm GeV/\mathit{c})^2$; charged particles from vector mesons such as ρ and $\rm K^*$ peak at ≈ 0.04 $(\rm GeV/\mathit{c})^2$; a peak at ≈ 0.008 $(\rm GeV/\mathit{c})^2$ is expected from two-body decays of baryons with very low Q values. This effect is especially important for the first momentum bin.

The results of the six measurements are listed in Table 1 together with statistical and systematic uncertainties, the latter calculated as the sum in quadrature of the uncertainties coming from the Monte Carlo statistics used to perform the test on the background shapes and the 100% uncertainties on the extra offset found in the same test. The comparison between data and Monte Carlo of the signal shape is shown in Figure 1b). The distributions shown are calculated, once the background is subtracted from the data, by normalizing the integrals in each momentum bin to unity and adding them with the weights determined as described in Section 5 and listed in Table 4.

4 Reconstruction of $\rm D^{*+} \to D^0\pi^+$, $\rm D^0 \to K^-\pi^+$

The events are divided in two hemispheres by the plane orthogonal to the thrust axis. Tracks with momentum between 1 and 4 GeV/c are π_s candidates. Two oppositely charged tracks are added with kaon mass assignment for the track with charge opposite

to the π_s and pion mass for the other track. The two tracks are retained if the decay angle of the kaon in the D^0 rest frame, θ^*_K, satisfies $|\cos\theta^*_K| < 0.8$. The $K^-\pi^+$ invariant mass is required to be in the range $1.835 - 1.895$ GeV/c^2. The mass differences $\Delta M = M(K\pi\pi_s) - M(K\pi)$ are shown in Figure 3 in π_s momentum slices of 0.5 GeV/c. The number of candidates is counted in the ΔM region between 0.1435 and 0.1475 GeV/c^2. The background is estimated from data using ΔM shapes taken from an event mixing method [5].

The background-subtracted number of observed $D^{*+} \to D^0\pi^+$, $D^0 \to K^-\pi^+$ decays in each momentum bin is shown in the third column of Table 1, together with the statistical uncertainties and the systematic uncertainties associated with the background subtraction.

5 Measurement of $B(D^0 \to K^-\pi^+)$

The number of selected D^{*+} decaying to $D^0\pi^+$, $N_{D^{*+}\to D^0\pi^+}$, determined in the inclusive analysis and the number of D^{*+} decays reconstructed through the $D^{*+} \to D^0\pi^+$, $D^0 \to K^-\pi^+$ decay chain, $N_{D^0\to K^-\pi^+}$, allow the determination of the branching fraction for $D^0 \to K^-\pi^+$ for each momentum bin:

$$B(D^0 \to K^-\pi^+) = \frac{N_{D^0\to K^-\pi^+}}{N_{D^{*+}\to D^0\pi^+}} \cdot \frac{\epsilon^{\rm incl}}{\epsilon^{\rm excl}} \ .$$

In this relation $\epsilon^{\rm incl}$ and $\epsilon^{\rm excl}$ are, respectively, the selection efficiencies for the inclusive and exclusive analyses and are calculated by Monte Carlo. The results obtained are shown in Table 2.

Systematic effects on the measurement are now discussed and the correlation matrix of the results in the six momentum bins is given. This correlation matrix is used to weight the six measurements, minimizing the total error. For the inclusive analysis the systematic errors are related to the description of the p_T^2 shape of the signal and the adequacy of the parameterization used to describe the background. In the exclusive analysis the contributions come from the efficiency calculation and the background subtraction.

The first contribution related to the p_T^2 shape of the signal comes from the relative fraction of c, b and gluon splitting events. The uncertainty is estimated by varying the parameters $P(c \to D^{*+})/P(b \to D^{*+})$, ε_c, ε_b and f_g/f_c within their errors. These variations affect both the relative fractions of the signal sources and the correction factors to the theoretical shapes, calculated using the measured and predicted $\theta_{D^{*+},\rm jet}$ distributions with the new input fractions. The effects in the six bins are fully correlated.

The decay angle of the π_s in the D^{*+} rest frame affects the p_T^2 distributions. The parameter α has been varied within the quoted errors. The resulting uncertainties in the six momentum bins are fully correlated.

The angle between the D^{*+} and the jet is measured in data using the fully reconstructed D^{*+}'s. The correction factors applied to the Monte Carlo predictions are affected by the statistical errors (of data and Monte Carlo) on the measurement. The errors have been propagated by randomly generating one hundred sets of the ratio of data to Monte Carlo in the $\theta_{D^{*+},\rm jet}$ distributions. The generation is done according to Gaussian distributions with means equal to the measured ratios and widths equal to the total errors. The p_T^2

corrections have been applied, repeating the fits one hundred times and the root mean squares of the results obtained are taken as systematic errors. The errors in the six momentum bins are partially correlated; the fluctuations induced in the measured ratios affect the six momentum bins differently because the dependence of $\theta_{\mathrm{D}^{*+},\mathrm{jet}}$ on p_{T}^2 varies with the π_s momentum. The correlation matrix is then determined by computing the covariance matrix in the one hundred fits.

The parameterization of the background is tested on Monte Carlo events from which the π_s tracks have been removed. The uncertainty from Monte Carlo statistics and 100% of the additional correction applied are summed in quadrature to estimate the uncertainties coming from this source. The errors for the six momentum bins are taken to be uncorrelated.

Low Q-value decays such as $\Sigma(1385) \to \Sigma\pi$, $\Xi \to \Lambda\pi$, or $\Sigma_{\mathrm{c}}(2455) \to \Lambda_{\mathrm{c}}\pi$ can fake the slow pion signal. The effect is calculated by examining tracks coming from baryon decays in the π_s-less Monte Carlo sample. The abundance of these tracks is varied by $\pm 10\%$ and the relative variation on the fit results is taken as systematic error. These errors are fully correlated for the six momentum bins.

The inclusive selection efficiency is determined from Monte Carlo events. The limited statistics used leads to an uncorrelated error for the six momentum bin. The efficiency depends on the jet content, if the D^0 decays to all neutrals the charge multiplicity requirement tends to give a lower efficiency. The uncertainties due to this source are evaluated by varying the $\mathrm{D}^0 \to \bar{\mathrm{K}}^0(n)\pi^0(m)\gamma$ branching fraction ($5.0 \pm 0.4\%$ [15]) within errors. This source is fully correlated in the six momentum bins.

The background subtraction in the exclusive channel is tested by using the predictions of the mixed events for candidates in the upper sideband of the $\mathrm{K}^-\pi^+$ invariant mass ($M(\mathrm{K}\pi) > 2.1$ GeV/c^2) and comparing them to the corresponding sample in the data. The agreement is good and the statistical uncertainties from the comparison are taken as a source of systematic errors. The main contributions, however, arise from the statistics of the sample of candidates in the data on the upper sideband of the ΔM distribution and from the statistics of the sample of mixed events used to determine the rates of combinatorial background in the six momentum bins. These are taken to be uncorrelated between the six momentum bins.

The efficiencies on the exclusive channel are determined from Monte Carlo events. The statistical errors are taken as uncorrelated systematic errors in the six momentum bins. The main systematic effects are due to the cuts on $\mathrm{K}^-\pi^+$ mass and ΔM. Radiative effects in D^0 decay are included in the efficiency calculation by using the PHOTOS generator [16]. The overall effect is a relative 1.9% increase of the branching fraction. The uncertainty on this calculation is neglected.

The tails of the mass and p_{T}^2 distributions are caused predominantly by nuclear interaction. The probability for one particle to undergo a nuclear interaction in the matter of the detector is assigned a relative uncertainty of 10%, based on a study of $\mathrm{Z} \to \tau^+\tau^-$ decays. The resulting uncertainties on the branching fractions are taken to be fully correlated in the six momentum bins.

A summary of the systematic errors on the measurement is given in Table 3. The overall correlation matrix for the six measurements is shown in Table 4. The six measurements are weighted such that the total error is minimized. The weight for each

momentum bin is computed as the sum of the corresponding row divided by the sum of all the elements of the inverted covariance matrix. The results are shown in the third column of Table 4. The result is

$$B(\mathrm{D}^0 \to \mathrm{K}^-\pi^+) = (3.90 \pm 0.09 \pm 0.12)\% \ .$$

The analysis is performed for various values of jet masses Y_{cut}. The results are shown in Figure 4. The chosen value $Y_{\mathrm{cut}} = 0.0024$ yields the smallest total uncertainty. The stability of the branching fraction as a function of the π_s momentum is very good for all Y_{cut} values.

6 Conclusions

The decay $\mathrm{D}^0 \to \mathrm{K}^-\pi^+$ has been studied in a sample of hadronic Z decays recorded with the ALEPH detector from 1991 to 1994. Fully reconstructed $\mathrm{D}^{*+} \to \mathrm{D}^0\pi^+$, $\mathrm{D}^0 \to \mathrm{K}^-\pi^+$ decays have been analysed together with the inclusive $\mathrm{D}^{*+} \to \mathrm{D}^0\pi^+$ process, yielding $B(\mathrm{D}^0 \to \mathrm{K}^-\pi^+) = (3.90 \pm 0.09 \pm 0.12)\%$, agreeing with and improving on previous measurements [1, 5, 8, 17, 18].

Acknowledgement

We wish to congratulate our colleagues in the CERN accelerator divisions for successfully operating the LEP storage ring. We are grateful to the engineers and technicians in all our institutions for their contribution towards ALEPH's success. Those of us from non-member countries thank CERN for its hospitality.

References

[1] S. Abachi *et al.* (HRS Collaboration), Phys. Lett. B 205 (1988) 411.

[2] D. Decamp *et al.* (ALEPH Collaboration), Nucl. Instr. Methods A 294 (1990) 121.

[3] D. Buskulic *et al.* (ALEPH Collaboration), Nucl. Instr. Methods A 360 (1995) 481.

[4] D. Decamp *et al.* (ALEPH Collaboration), Z. Phys. C53 (1992) 1.

[5] D. Decamp *et al.* (ALEPH Collaboration), Phys. Lett. B 266 (1991) 218.

[6] P. Baringer *et al.* (HRS Collaboration), Phys. Lett. B 206 (1988) 551.

[7] P. Abreu *et al.* (DELPHI Collaboration), Phys. Lett. B 252 (1990) 140.

[8] D. S. Akerib *et al.* (CLEO Collaboration), Phys. Rev. Lett. 71 (1993) 3070.

[9] W. Bartel *et al.* (JADE Collaboration), Z. Phys. C33 (1986) 23.

[10] D. Buskulic *et al.* (ALEPH Collaboration), Z. Phys. C62 (1994) 1.

[11] R. Akers *et al.* (OPAL Collaboration), Phys. Lett. B 353 (1995) 595.

[12] R. Akers *et al.* (OPAL Collaboration), Z. Phys. C67 (1995) 27.

[13] C. Peterson, D. Schlatter, I. Schmitt and P. M. Zerwas, Phys. Rev. D 27 (1983) 105.

[14] D. Buskulic *et al.* (ALEPH Collaboration), Z. Phys. C62 (1994) 179.

[15] R.M. Barnett *et al.* (Particle Data Group), Phys. Rev. D 54 (1996) 1.

[16] E. Barberio, R. Van Eijk and Z. Wąs, Comp. Phys. Comm. 66 (1991) 115.

[17] J. Adler *et al.* (MARK III Collaboration), Phys. Rev. Lett. 60 (1988) 89.

[18] H. Albrecht *et al.* (ARGUS Collaboration), Phys. Lett. B340 (1995) 125.

Table 1: Results of the inclusive and exclusive analyses performed in the six ranges of the soft pion momentum. In each case the first error is statistical and the second systematic.

Momentum range (GeV/c)	$N_{\mathrm{D}^{*+}\to\mathrm{D}^0\pi^+}$	$N_{\mathrm{D}^0\to\mathrm{K}^-\pi^+}$
1.0−1.5	79038.2±2021.9±12018.0	2472.9±55.5±11.0
1.5−2.0	56393.2±1140.4± 921.6	1558.3±41.4± 5.4
2.0−2.5	35303.4± 855.8 ± 842.2	913.8 ±30.9± 2.8
2.5−3.0	12287.8± 674.7 ± 535.1	321.5 ±18.2± 1.3
3.0−3.5	3497.4 ± 499.2 ± 630.4	115.7 ±10.9± 0.7
3.5−4.0	192.4 ± 366.8 ± 401.5	9.8 ± 3.3 ± 0.4

Table 2: Measured branching fractions in the six bins of the soft pion momentum. In the third and fourth columns are shown the efficiencies for the inclusive and exclusive analyses, respectively, together with the errors due to the Monte Carlo statistics.

Momentum range (GeV/c)	$B(\mathrm{D}^0\to\mathrm{K}^-\pi^+)$	ϵ^{incl}	ϵ^{excl}
1.0−1.5	(4.400±0.150±1.041)%	(72.77±0.10)%	(51.75±0.41)%
1.5−2.0	(3.990±0.133±0.139)%	(73.10±0.12)%	(50.62±0.46)%
2.0−2.5	(3.768±0.157±0.150)%	(73.13±0.15)%	(50.23±0.58)%
2.5−3.0	(3.758±0.296±0.206)%	(72.26±0.23)%	(50.31±0.86)%
3.0−3.5	(5.010±0.857±1.228)%	(72.15±0.42)%	(47.64±1.51)%
3.5−4.0	(7.34 ± 14.2 ±19.4)%	(71.64±1.23)%	(49.71±4.31)%

Table 3: The principal sources of systematic errors for the branching fraction measurement. The errors are absolute.

Error source	Systematic error
sample composition	0.011%
alignment of the D^{*+}	0.010%
$\theta_{\mathrm{D}^{*+},\mathrm{jet}}$	0.086%
background subtraction in the inclusive analysis	0.061%
baryon rate	0.008%
efficiency of the inclusive analysis	0.006%
background subtraction in the exclusive analysis	0.008%
efficiency of the exclusive analysis, MC statistics	0.025%
mass cuts	0.005%
yield of nuclear interactions	0.040%
total	0.117%

Table 4: Total error correlation matrix of the measurements in the six momentum bins. The weight of each measurement when the results are combined is listed in the last column.

momentum bin (GeV/c)	Correlation matrix						weight
$1.0-1.5$	1	0.011	0.008	0.003	0.001	0.001	0.019
$1.5-2.0$		1	0.218	0.108	0.022	0.004	0.493
$2.0-2.5$			1	0.102	0.024	0.004	0.360
$2.5-3.0$				1	0.019	0.002	0.121
$3.0-3.5$					1	0.001	0.007
$3.5-4.0$						1	0

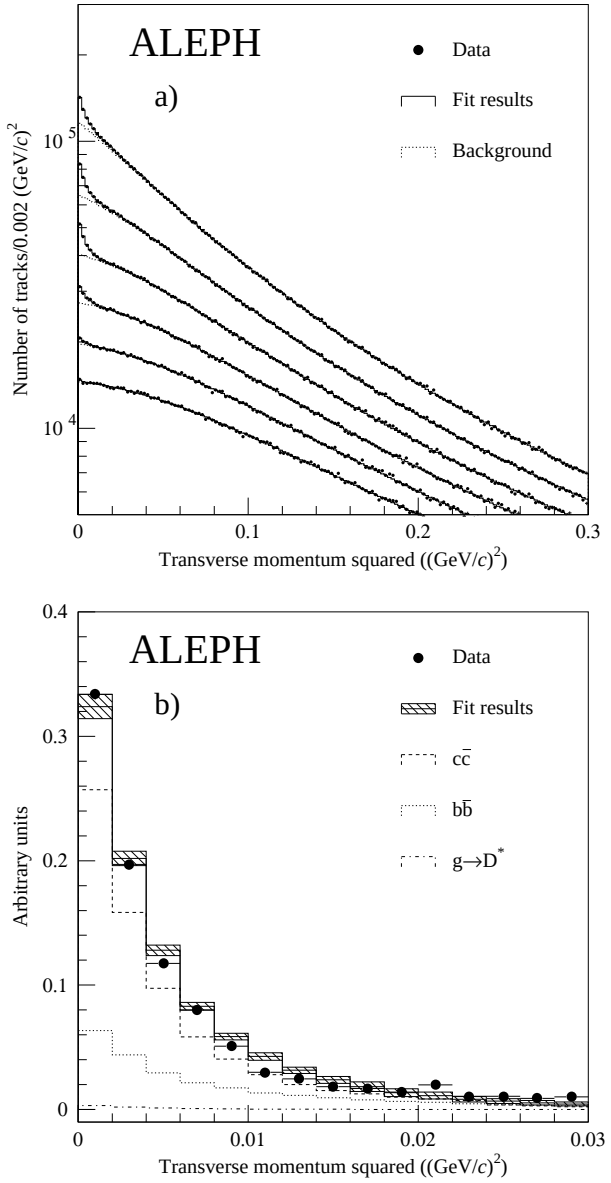

Figure 1: a) Transverse momentum squared of tracks in 0.5 GeV/c momentum bins from 1 GeV/c (uppermost) to 4 GeV/c. The signal peaks in the low-p_{T}^2 region. b) Signal p_{T}^2 distributions, determined as described in the text, are shown . The hatched rectangles represent the Monte Carlo prediction within errors. In the error the uncertainty concerning the offset on the rate is not included.

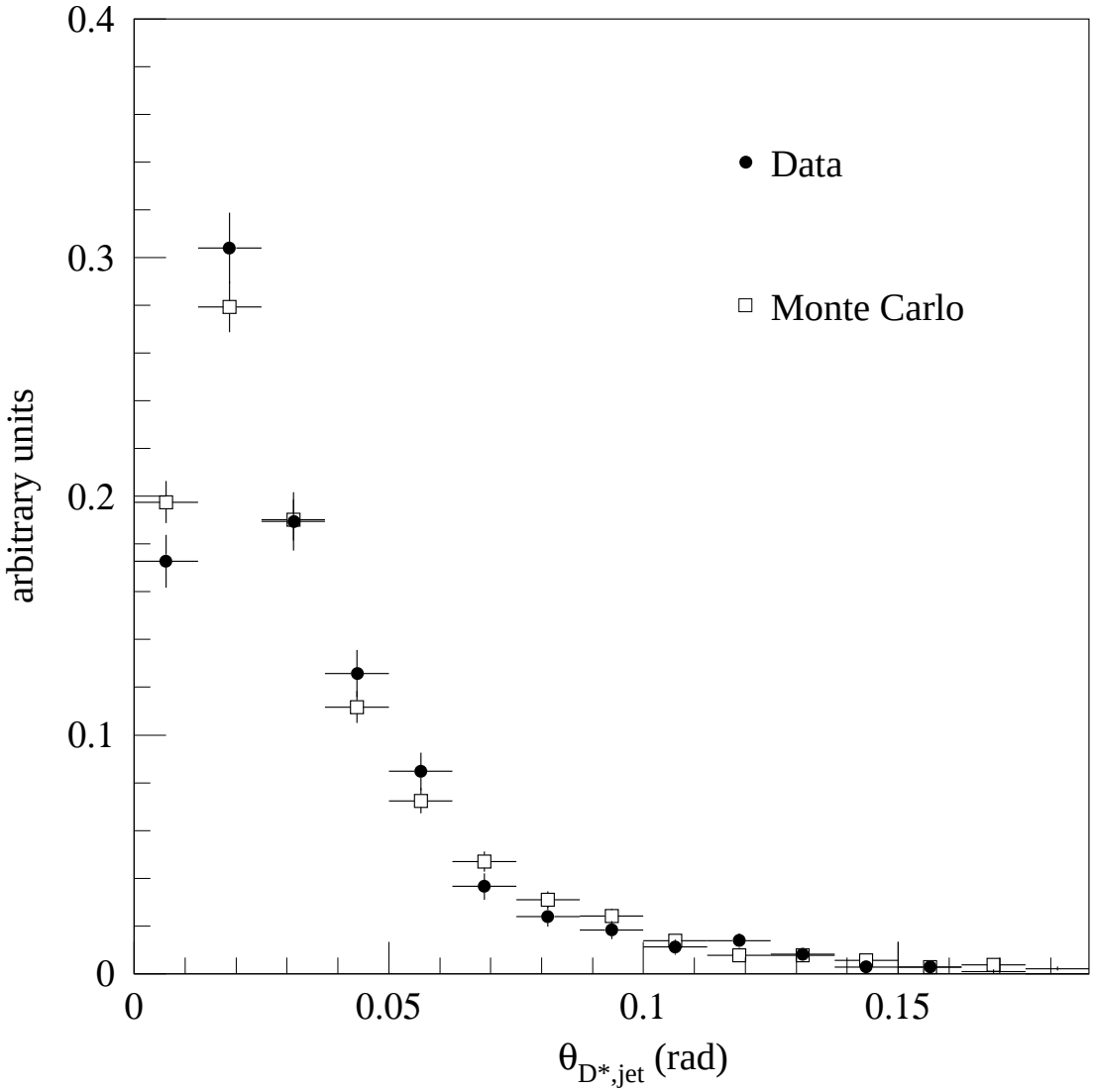

Figure 2: Distribution of the angle between the D^{*+} and the jet for signal events. The dots are the data and the open squares are the $q\bar{q}$ Monte Carlo events, normalized to the same area.

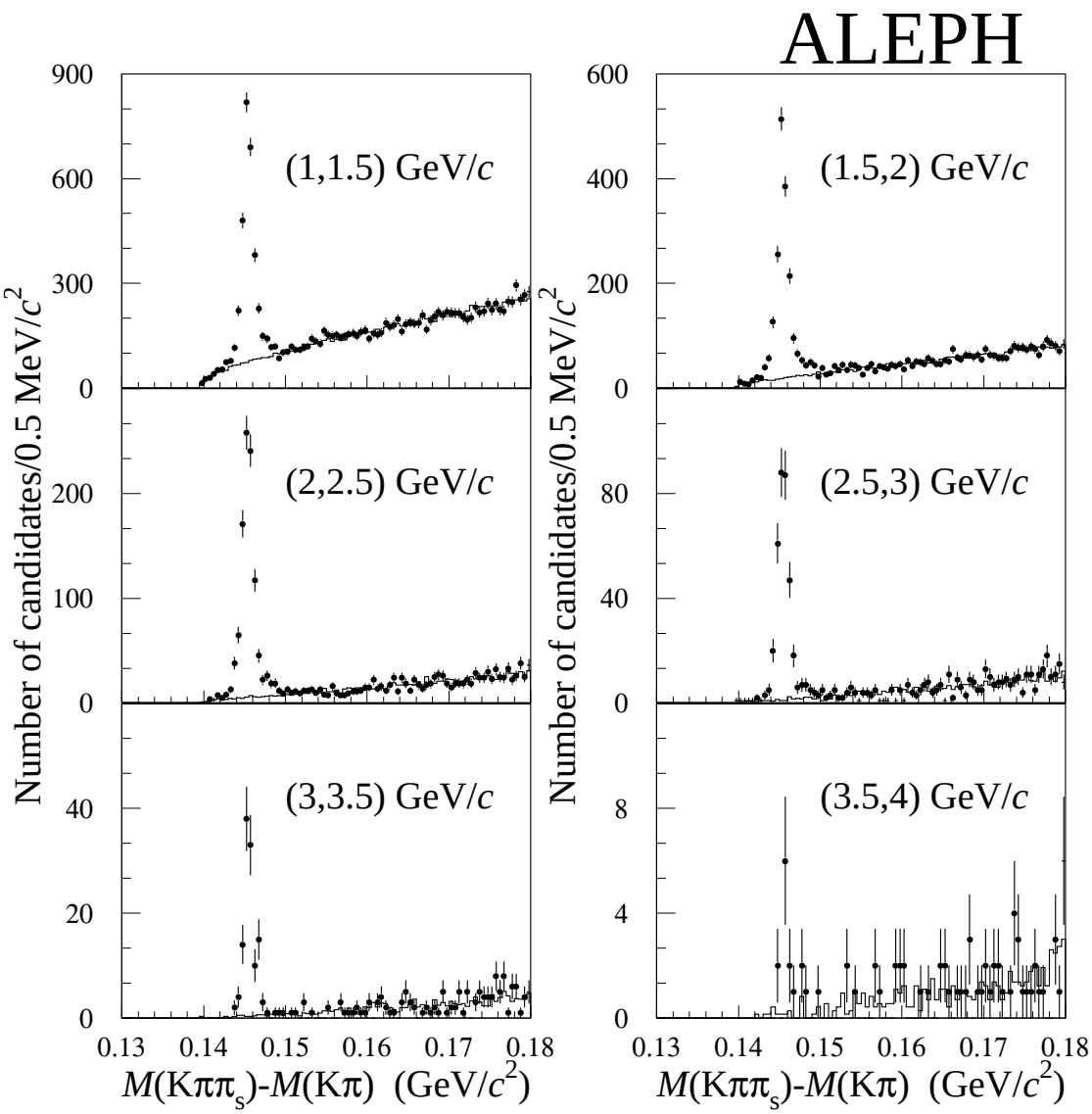

Figure 3: The ΔM distributions for the six 0.5 GeV/c slices in the π_s momentum. The dots are the data, and the histograms represent the background as described in the text.

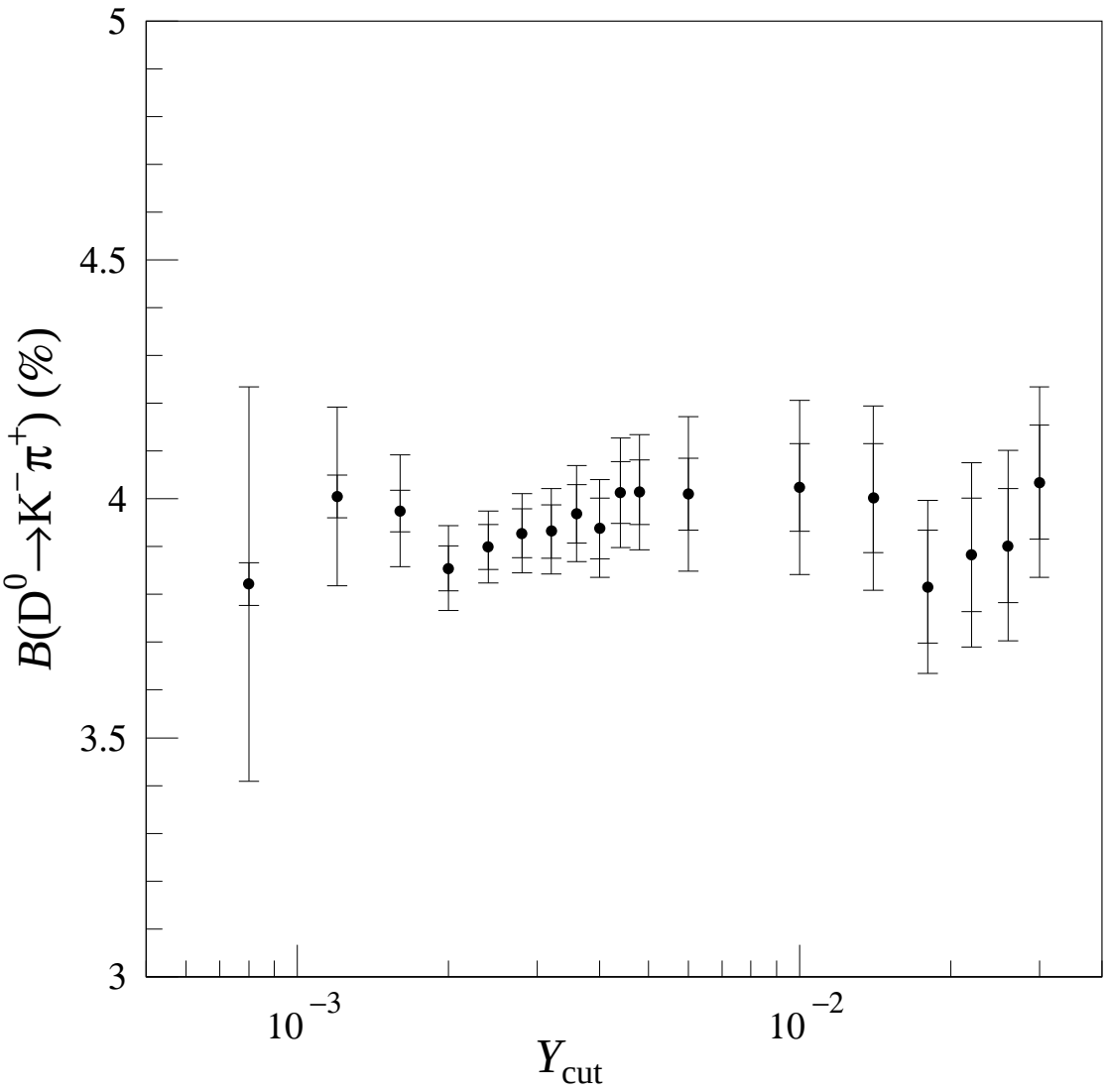

Figure 4: Measurements of $B(\mathrm{D}^0 \to \mathrm{K}^-\pi^+)$ as a function of the jet mass parameter Y_{cut}. The large error bars represent the total uncertainty, while the smaller ones indicate the statistical component of the error. The result for $Y_{\mathrm{cut}} = 0.0024$ has minimal total error.